Dumlupınar Üniversitesi Fen Bilimleri Enstitüsü Dergisi
Sayı: 17 Aralık 2008 ISSN - 1302 - 3055

EFFICIENT AND FAST FINITE ELEMENT VISCOELASTIC FLUID FLOW SIMULATION EFFORTS

Bayram ALAKUŞ*

*Department of Mechanical Engineering, Dumlupinar University, Kutahya

Geliş Tarihi:21.11.2008 *Kabul Tarihi: 19.12.2008*

ABSTRACT

In this research, we provide finite element computational developments to predict the flow behavior of a viscoelastic fluid flow. The developments predict the velocity, pressure, and polymeric stress by modeling the conservation laws (e.g. mass and momentum) of the flow field coupled with constitutive equations for polymeric stress field. The simulations target a variety of viscoelastic models (e.g. Upper-Convected-Maxwell Model, Oldroyd-B model and Giesekus model) to provide a fundamental understanding of the elastic effects on the flow field. To solve the complex coupled nonlinear equations of the mathematical model described above, a combination of Newton linearization and the Galerkin and Streamline-Upwinding-Petrov-Galerkin (SUPG) finite element procedures are employed to accurately capture the representative physics.

Key Words: *EVSS-1 ve EVSS-2 Finite element method, viscoelastic flows, GMRES solver*

VİSKOELASTİK AKIŞKAN AKIŞININ SONLU ELEMANLAR METODU İLE HIZLI VE ETKİLİ SİMULASYONU

ÖZET

Bu çalışmada, sonlu elemanlar metodunu kullanarak viskoelastik akışkanların etkili ve hızlı olarak sayısal çözümü için gerekli algoritma verildi. Akış alanına ait hız, basınç, Newtonian ve polimerik gerilmeler çözüm olarak sunuldu. Temel korunum yasaları çeşitli viskoelastik modeller (e.g. Upper-Convected-Maxwell Model, Oldroyd-B model and Giesekus model) kullanılarak matematiksel model elde edildi. Bu model, Newton lineerleştirme metodu, SUPG sonlu elemanlar metodu ve GMRES iterative çözüm tekniği kullanılarak çözümler elde edildi.

Anahtar Kelimeler: *EVSS-1 ve EVSS-2Sonlu elemanlar methodu, viskoelastik akışkanla, GMRES solver*

1.INTRODUCTION

Viscoelastic fluid flows are extremely difficult to handle computationally. The main feature of the constitutive equations is the convective character of the stress evolution. The difficulty is lessened considerably by even a small addition of the Newtonian solvent in EVSS formulation. Even so, one may expect the problems normally associated with an advective system to arise when discretization of the constitutive equation is performed. An additional feature introduced by the viscoelastic equations is their non-linearity. From the computational point of view, that property is a strong argument for solving the equations for stress and velocity in a coupled manner. The Newtonian model for the stress is easily incorporated into the momentum equations to yield some of the most commonly seen forms of the Navier-Stokes equations. The viscoleastic models on the other hand, necessitate treatment of the extra stress tensor and rate-of-strain tensor as separate variables.

The main objective of the current effort is to develop a computational formulation that accurately captures the flow characteristics by making use of a consistent upwinding method (the SUPG formulation) and a

fast iterative solver (the GMRES solver). Previous commercial softwares use inconsistent upwinding methods (the SU formulation) which are unable to represent correctly the physics of the flow field at high Deborah numbers.

The contributions of the current work include the first research efforts to employ Newton's linearization, Streamline-Upwinding-Petrov-Galerkin (SUPG) Method, Elastic-Viscous-Split-Scheme (EVSS-2) and the preconditioned Generalized Minimal Residual (GMRES) solver for obtaining the solution of viscoelastic fluid flows.

Additionally, the current formulation provides a comparative study of two benchmark problems with strong singularities either because of the geometry with sharp corners or because of the imposition of the boundary conditions for the viscoelastic flows.

2. GOVERNING DIFFERENTIAL EQUATIONS

The continuity equation (conservation of mass) and the equation of motion (conservation of momentum) for flow field are;

$$\frac{\partial \rho_{\mathrm{f}}}{\partial t} + \nabla \cdot \left(\rho_{\mathrm{f}} \boldsymbol{v}_{\mathrm{f}}\right) = 0 \tag{1}$$

$$\frac{\partial \left(\rho \boldsymbol{v}\right)}{\partial t} + \nabla \cdot \left(\rho \boldsymbol{v}\boldsymbol{v}\right) = \nabla \cdot \boldsymbol{\sigma} + \rho \boldsymbol{g} \tag{2}$$

where $\boldsymbol{\sigma}$ is the total fluid stress tensor which is comprised of the pressure and viscous and polymeric stresses, and $\boldsymbol{g}$ is the gravitational body force per unit mass, ρ is the density.

The constitutive equation for a Newtonian fluid is defined as:

$$\boldsymbol{\tau}_{\mathrm{f}} = \eta\left(\nabla \boldsymbol{v}_{\mathrm{f}} + \left(\nabla \boldsymbol{v}_{\mathrm{f}}\right)^{\mathrm{T}}\right) \tag{3}$$

where $\boldsymbol{\tau}_{\mathrm{f}}$ is the total extra stress, $\dot{\boldsymbol{\gamma}} = \nabla \boldsymbol{v}_{\mathrm{f}} + \left(\nabla \boldsymbol{v}_{\mathrm{f}}\right)^{\mathrm{T}}$ is the rate of strain tensor, η is the viscosity.

For the constitutive equations of non-Newtonian fluids (viscoelastic fluids), let $\boldsymbol{\sigma}$ denote the Cauchy (total) stress tensor, then the extra stress $\boldsymbol{T}_{\mathrm{f}}$ is defined by $\boldsymbol{\sigma}_{\mathrm{f}} = -p\boldsymbol{I} + \boldsymbol{T}_{\mathrm{f}}$,where p is the indeterminate pressure and the extra-stress $\boldsymbol{T}_{\mathrm{f}}$ is given by a differential constitutive model [1] as:

a) Upper-Convected Maxwell (UCM) Model

$$\boldsymbol{T}_{\mathrm{f}} + \lambda_1\left(\frac{\partial \boldsymbol{T}_{\mathrm{f}}}{\partial t} - \nabla \boldsymbol{v}_{\mathrm{f}}^{\mathrm{T}} \cdot \boldsymbol{T}_{\mathrm{f}} - \boldsymbol{T}_{\mathrm{f}} \cdot \nabla \boldsymbol{v}_{\mathrm{f}}\right) = -\eta\left(\nabla \boldsymbol{v}_{\mathrm{f}} + \nabla \boldsymbol{v}_{\mathrm{f}}^{\mathrm{T}}\right) \tag{4}$$

where by definition $\boldsymbol{T}_{(1)} = \frac{\partial \boldsymbol{T}_{\mathrm{f}}}{\partial t} - \nabla \boldsymbol{v}_{\mathrm{f}}^{\mathrm{T}} \cdot \boldsymbol{T}_{\mathrm{f}} - \boldsymbol{T}_{\mathrm{f}} \cdot \nabla \boldsymbol{v}_{\mathrm{f}}$ is the Upper-Convected derivative of the polymeric stress, $\boldsymbol{v}_{\mathrm{f}}$ is the velocity vector, λ_1 is relaxation time and η is the total viscosity.

b) Oldroyd-B Model

$$\boldsymbol{T}_{\mathrm{f}} + \lambda_1\left(\frac{\partial \boldsymbol{T}_{\mathrm{f}}}{\partial t} - \nabla \boldsymbol{v}_{\mathrm{f}}^{\mathrm{T}} \cdot \boldsymbol{T}_{\mathrm{f}} - \boldsymbol{T}_{\mathrm{f}} \cdot \nabla \boldsymbol{v}\right) = -\eta\left[\left(\nabla \boldsymbol{v}_{\mathrm{f}} + \nabla \boldsymbol{v}_{\mathrm{f}}^{\mathrm{T}}\right) + \lambda_2 \dot{\boldsymbol{\gamma}}_{(1)}\right] \tag{5}$$

where $\dot{\boldsymbol{\gamma}}_{(1)} = \frac{\partial \dot{\boldsymbol{\gamma}}}{\partial t} - \nabla \boldsymbol{v}_{\mathrm{f}}^{\mathrm{T}} \cdot \dot{\boldsymbol{\gamma}} - \dot{\boldsymbol{\gamma}} \nabla \boldsymbol{v}_{\mathrm{f}}$ is the Upper-Convected derivative of the rate-of-strain tensor, $\boldsymbol{v}_{\mathrm{f}}$ is the velocity vector, λ_1 is relaxation time, λ_2 is retardation time and η is the total viscosity [1].

c) Giesekus Model

The extra-stress $\boldsymbol{T}_{\mathrm{f}}$ is decomposed of a solvent viscous stress tensor $\boldsymbol{T}_2$ and a polymeric stress tensor $\boldsymbol{\tau}_1$ as $\boldsymbol{T}_{\mathrm{f}} = \boldsymbol{\tau}_1 + \boldsymbol{T}_2$ and

$$\boldsymbol{\tau}_1 + \lambda_1\left(\frac{\partial \boldsymbol{\tau}_1}{\partial t} - \nabla \boldsymbol{v}_{\mathrm{f}}^{\mathrm{T}} \cdot \boldsymbol{\tau}_1 - \boldsymbol{\tau}_1 \cdot \nabla \boldsymbol{v}\right) + \alpha \frac{\lambda_1}{\eta_1}\left\{\boldsymbol{\tau}_1 \boldsymbol{\tau}_1\right\} = \eta_1\left(\nabla \boldsymbol{v}_{\mathrm{f}} + \nabla \boldsymbol{v}_{\mathrm{f}}^{\mathrm{T}}\right)$$

$$\boldsymbol{T}_2 = \eta_2\left(\nabla \boldsymbol{v}_{\mathrm{f}} + \nabla \boldsymbol{v}_{\mathrm{f}}^{\mathrm{T}}\right) \tag{6}$$

where η_2 is the solvent viscosity, η_1 is the polymeric viscosity and $\eta = \eta_1 + \eta_2$ is the total viscosity. α is a dimensionless Giesekus model mobility factor. When $\alpha = 0.5$, the model is called Giesekus-Leonov model and it can be used for the simulations of the most of viscoelastic fluid flows [1].

d) Phan-Thien and Tanner (PTT) Model

The extra-stress $\boldsymbol{T}_f$ is decomposed of a solvent viscous stress tensor $\boldsymbol{T}_2$ and a polymeric stress tensor $\boldsymbol{T}_1$ as $\boldsymbol{T}_f = \boldsymbol{T}_1 + \boldsymbol{T}_2$ and

$$\left[1 + \frac{\varepsilon_m \lambda_1}{\eta_1}\mathrm{trace}(\boldsymbol{T}_1)\right]\boldsymbol{T}_1 + \lambda_1\left(\frac{\partial \boldsymbol{T}_1}{\partial t} - \nabla \boldsymbol{v}_f^T \cdot \boldsymbol{T}_1 - \boldsymbol{T}_1 \cdot \nabla \boldsymbol{v}\right) = \eta_1\left(\nabla \boldsymbol{v}_f + \nabla \boldsymbol{v}_f^T\right)$$

$$\boldsymbol{T}_2 = \eta_2\left(\nabla \boldsymbol{v}_f + \nabla \boldsymbol{v}_f^T\right) \qquad (7)$$

where, ε_m is a model parameter and λ_1 is the relaxation time [1].

The Elastic-Viscous-Split-Stress (EVSS) Formulation

The EVSS formulation of the UCM and Oldroyd-B models is derived based on the change of variables as follows. Define the elastic stress as

$$\boldsymbol{T}_f = \boldsymbol{T}_1 + \eta\dot{\gamma} \quad \text{and}$$

$$\boldsymbol{T}_1 + \lambda_1\left(\boldsymbol{T}_{1(1)} - (1-\beta)\eta\dot{\gamma}_{(1)}\right) = 0 \qquad (8)$$

where β is the ratio of the retardation time to the relaxation time; $\beta = \lambda_2/\lambda_1$. When $\beta = 0$ the EVSS form of the UCM model is recovered.

Giesekus Model

For the EVSS formulation of Giesekus model, define the elastic stress as

$$\boldsymbol{\tau}_f = \boldsymbol{T}_1 + \eta_1\dot{\gamma} \quad \text{and}$$

$$\boldsymbol{T}_1 + \lambda_1\left(\boldsymbol{T}_{1(1)} - (1-\beta)\eta\dot{\gamma}_{(1)}\right) + \alpha\frac{\lambda_1}{(1-\kappa)\eta_1}\{\boldsymbol{T}_1 \cdot \boldsymbol{T}_1\} - \alpha\lambda_1(\boldsymbol{T}_1 \cdot \dot{\gamma} + \dot{\gamma} \cdot \boldsymbol{T}_1) + \alpha\lambda_1(1-\kappa)\eta\dot{\gamma} \cdot \dot{\gamma} = 0 \qquad (9)$$

where $\kappa = \eta_2/\eta$.

3. COMPUTATIONAL FORMULATIONS: FINITE ELEMENT EQUATIONS

The weak forms of the mass, momentum, and constitutive equations are derived with the weighted residual method. The constitutive equations are weighted by the Streamline-Upwinding-Petrov-Galerkin (SUPG) [7] weighting functions to account for the presence of the convective terms and to stabilize the polymeric stress field, while continuity, momentum and rate of strain equations are weighted by Galerkin weighting functions. Details are overviewed next. To solve the finite element equations, the following steps are required for the weighted residual method:

1. Replace the flow variables by approximate finite element variables and then, obtain the residuals of the equations
2. Multiply the residuals by an appropriate weighting function and integrate over the element domain
3. Apply Divergence theorem to the total stress term in the momentum equations to reduce the order of integration (The weak form)
4. Impose the homogeneous natural boundary condition
5. Linearize the system by Newton's method
6. Obtain the element stiffness (Jacobian) matrix and the right hand side vector
7. Assemble the element stiffness matrices and the element right hand side vector

Momentum Equations:

When steps 1 and 2 are applied to the averaged momentum equations, we get

$$\int_\Omega \left[\nabla P - \nabla \boldsymbol{T}_1 - \eta\nabla^2 \boldsymbol{v}_f - \eta\nabla \cdot \nabla^T \boldsymbol{v}_f + \rho_f \frac{\partial \boldsymbol{v}_f}{\partial t}\right] \boldsymbol{w}_m \, d\Omega = 0 \qquad (10)$$

where $\sigma = P\boldsymbol{\delta} - \boldsymbol{T}_1 - \eta\left(\nabla \boldsymbol{v}_\mathrm{f} + \nabla^\mathrm{T} \boldsymbol{v}_\mathrm{f}\right)$ is the total stress tensor $\boldsymbol{\delta}$ is the unit tensor, $\boldsymbol{w}_m$ is the weighting functions. The 3rd step of the computational procedure is implemented for the total stress field as follows: Let $\boldsymbol{\sigma}$ represent the total stress tensor.

$$\int_\Omega \nabla \cdot (\boldsymbol{\sigma} w) \mathrm{d}\Omega = \int_\Omega (\nabla \cdot \boldsymbol{\sigma}) w \mathrm{d}\Omega + \int_\Omega \boldsymbol{\sigma} \nabla w \mathrm{d}\Omega \tag{11}$$

Now, the imposition of the divergence theorem or the Green theorem gives:

$$\int_\Omega \nabla \cdot (\boldsymbol{\sigma} w) \mathrm{d}\Omega = \int_\Gamma (\mathbf{n} \cdot \boldsymbol{\sigma}) w \mathrm{d}\Gamma \tag{12}$$

Combining Eqns. (11) and (12) yields

$$\int_\Omega (\nabla \cdot \boldsymbol{\sigma}) w \mathrm{d}\Omega = -\int_\Omega \boldsymbol{\sigma} \cdot \nabla w \mathrm{d}\Omega + \int_\Gamma (\mathbf{n} \cdot \boldsymbol{\sigma}) \cdot w \mathrm{d}\Gamma \tag{13}$$

Finally by making use of the homogeneous boundary condition produces the desired result of the weak form as

$$\int_\Omega (\nabla \cdot \boldsymbol{\sigma}) w \mathrm{d}\Omega = -\int_\Omega \boldsymbol{\sigma} \cdot \nabla w \mathrm{d}\Omega \tag{14}$$

Rate of Strain Tensor:

Steps 1 and 2 result in the following equation:

$$\int_\Omega \left[\boldsymbol{D} - \frac{1}{2}\left(\nabla \boldsymbol{v}_\mathrm{f} + \nabla^\mathrm{T} \boldsymbol{v}_\mathrm{f}\right) \right] \cdot \boldsymbol{w}_d \mathrm{d}\Omega = 0 \tag{15}$$

where $\boldsymbol{w}_d$ are the weighting functions corresponding to the rate-of-strain tensor.

Continuity Equation:

$$\int_\Omega \left(\frac{\partial u}{\partial x} + \frac{\partial v}{\partial y} \right) w_p \mathrm{d}\Omega = 0 \tag{16}$$

where w_p is the weighting function corresponding to the pressure field.

Constitutive Equations :

a) UCM and Oldroyd-B Models

$$\int_\Omega \Big[\boldsymbol{T}_1 + \lambda_1 \left(\frac{\partial \boldsymbol{T}_1}{\partial t} + 2\eta(1-\beta)\frac{\partial \boldsymbol{D}}{\partial t} \right) + \lambda_1 \big[(\boldsymbol{v}_\mathrm{f} \cdot \nabla)(\boldsymbol{T}_1 + 2\eta(1-\beta)\boldsymbol{D}) - (\boldsymbol{T}_1 + 2\eta(1-\beta)\boldsymbol{D}) \cdot \nabla \boldsymbol{v}_\mathrm{f} -$$
$$\left(\nabla \boldsymbol{v}_\mathrm{f}\right)^\mathrm{T} \left(\boldsymbol{T}_1 + 2\eta(1-\beta)\boldsymbol{D}\right) \big] \cdot \boldsymbol{w}_s \mathrm{d}\Omega = 0 \tag{17}$$

When β is equal to zero, the UCM Model recovered. The Streamline-Upwind Petrov-Galerkin (SUPG) formulation proposed by Brooks and Hughes [2] is implemented as follows:

$$\boldsymbol{w}_\mathrm{s} = \boldsymbol{w} + \psi^\mathrm{h} \boldsymbol{v}_\mathrm{f} \cdot \nabla \boldsymbol{w} \tag{18}$$

Following Shakib [3], we have

$$\psi^\mathrm{h} = \frac{\partial \chi_i}{\partial x_j} \frac{\partial \chi_i}{\partial x_k} v_i v_j \tag{19}$$

where i =1,2,3, ….,9 , j,k 1,2 in two-spatial dimensions. Here v_k are the components of the velocity vector and χ_i are the local coordinates (ξ, ζ) on the quadrilateral element.

b) Giesekus Model

$$\int_\Omega \Big[\boldsymbol{T}_1 + \lambda_1 \left(\frac{\partial \boldsymbol{T}_1}{\partial t} + 2\eta(1-\beta)\frac{\partial \boldsymbol{D}}{\partial t} \right) + \alpha \frac{\lambda_1}{\eta_1} \left\{ \left(\boldsymbol{T}_1 + 2\eta(1-\beta)\boldsymbol{D}\right)\left(\boldsymbol{T}_1 + 2\eta(1-\beta)\boldsymbol{D}\right) \right\}$$
$$\lambda_1 \big[(\boldsymbol{v}_\mathrm{f} \cdot \nabla)(\boldsymbol{T}_1 + 2\eta(1-\beta)\boldsymbol{D}) - (\boldsymbol{T}_1 + 2\eta(1-\beta)\boldsymbol{D}) \cdot \nabla \boldsymbol{v}_\mathrm{f} -$$
$$\left(\nabla \boldsymbol{v}_\mathrm{f}\right)^\mathrm{T} \left(\boldsymbol{T}_1 + 2\eta(1-\beta)\boldsymbol{D}\right) \big] \cdot \boldsymbol{w}_s \mathrm{d}\Omega = 0 \tag{20}$$

c) PTT Model

$$\int_{\Omega}\left[\left[1+\frac{\varepsilon_{\mathrm{m}}\lambda_1}{\eta_1}\mathrm{trace}(\boldsymbol{T}_1)\right]\boldsymbol{T}_1+\lambda_1\left(\frac{\partial \boldsymbol{T}_1}{\partial t}+2\eta\frac{\partial \boldsymbol{D}}{\partial t}\right)+\right.$$

$$\left.\lambda_1\left[(\boldsymbol{v}_{\mathrm{f}}\cdot\nabla)(\boldsymbol{T}_1+2\eta\boldsymbol{D})-(\boldsymbol{T}_1+2\eta\boldsymbol{D})\cdot\nabla\boldsymbol{v}_{\mathrm{f}}-(\nabla\boldsymbol{v}_{\mathrm{f}})^{\mathrm{T}}(\boldsymbol{T}_1+2\eta\boldsymbol{D})\right]\cdot\boldsymbol{w}_s\,\mathrm{d}\Omega=0 \qquad (21)$$

Newton's Linearization Method and Finite Element Equations

A mathematical model for a physical process is usually a set of Partial Differential Equations (PDE's) expressed in the general form of

$$\frac{\partial \mathbf{u}}{\partial t}=\mathbf{F}(\mathbf{u}(\mathbf{x},t)) \qquad (22)$$

where **u** (**x**, *t*) is the vector of field variables, **x** is the position vector, *t* is the time, and **F** is a nonlinear differential operator. This equation is defined on a domain Ω for some time, with initial conditions at $t = 0$ and boundary conditions on the boundaries of the domain ∂Ω. Solution requires a full simulation in space and time. Sometimes only the *steady-state* solutions are required; in that case, the time derivatives are zero and a spatial simulation for $\mathbf{F}(\mathbf{u}(\mathbf{x}))) = 0$ suffices.

An efficient steady-state solution procedure using a finite element/Newton algorithm is the finite element/Newton algorithm. Extensions to time-dependent equations are possible by temporal discretization and by adding an overall time integration loop in the solution procedure. The finite element/Newton algorithm has been used successfully to obtain the solution of complicated simulations including viscoelastic fluid flows (King et al [4]).

Partial differential equations are discretized and boundary conditions are applied with finite elements. For steady-state problems, these steps result in a nonlinear system of algebraic equations, written as

$$\mathbf{F}(\mathbf{u}(\mathbf{x}))=0 \qquad (23)$$

where the same notation for **F** is used for the discretized nonlinear differential operator. Newton's method is used to solve this nonlinear set through iteration as

for $k = 1 \rightarrow$ convergence solve

$$\mathbf{F}_{\mathbf{u}}^{k}\delta\mathbf{u}^{k}=-\mathbf{F}^{k}$$

$$\mathbf{u}^{k+1}=\mathbf{u}^{k}+\delta\mathbf{u}^{k} \qquad (24)$$

where $\mathbf{F}_{\mathbf{u}}^{k}$ is the Jacobian matrix at step *k* with entries $\left\{\mathbf{F}_{\mathbf{u}}^{k}\right\}_{ij}\equiv\left(\partial F_i/\partial u_j\right)^{k}$, and $\delta\mathbf{u}^{k}$ is the correction vector to the solution at step *k*. Newton's method is simply derived from a Taylor series expansion of the residual by keeping only the linear terms

$$\mathbf{F}^{k+1}\cong\mathbf{F}^{k}+\mathbf{F}_{\mathbf{u}}^{k}\delta\mathbf{u}^{k}=0 \qquad (25)$$

This method converges quadratically when the initial guess u_j^0 is close to the actual solution. A linear system of equations needs to be solved at each Newton iteration step

$$\mathbf{F}_{\mathbf{u}}^{k}\delta\mathbf{u}^{k}=-\mathbf{F}^{k} \qquad (26)$$

We implement Newton's Method to linearize the non-linear system of the governing equations as follows. Let

$$\boldsymbol{v}_{\mathrm{f}}=\boldsymbol{v}_{\mathrm{f}}^{/}+\boldsymbol{v}_{\mathrm{f}}^{o},\quad \boldsymbol{D}=\boldsymbol{D}^{/}+\boldsymbol{D}^{o},\quad \boldsymbol{T}_1=\boldsymbol{T}_1^{/}+\boldsymbol{T}_1^{o}\quad\text{and}\quad p=p^{/}+p^{o} \qquad (27)$$

where $\boldsymbol{v}_{\mathrm{f}}^{/}$, $\boldsymbol{D}^{/}$, $\boldsymbol{T}_1^{/}$ and $p^{/}$ are the unknowns to be solved, and $\boldsymbol{v}_{\mathrm{f}}^{0}$, $\boldsymbol{D}^{0}$, $\boldsymbol{T}_1^{0}$ and p^{0} are the starting guesses.

Finite Element Spaces

The flow domain Ω is discerized by means of quadrilateral finite elements. Let ***S***, ***D***, ***u***, *p* denote the corresponding approximation of $\boldsymbol{T}_1^{/}$, $\boldsymbol{D}^{/}$, $\boldsymbol{v}_{\mathrm{f}}^{/}$, and $p^{/}$. Then

$$\boldsymbol{v}_{\mathrm{f}}^{/}=\sum_{i=1}^{NN_q} q_i(x,y)\boldsymbol{u}_{\mathrm{i}}\ ,\ \boldsymbol{D}^{/}=\sum_{i=1}^{NN_q} q_i(x,y)\boldsymbol{D}_{\mathrm{i}}\ ,\ \boldsymbol{T}_1^{/}=\sum_{i=1}^{NN_q} q_i(x,y)\boldsymbol{S}_{\mathrm{i}}\ ,\ p^{/}=\sum_{i=1}^{NN_L} N_i(x,y)p_{\mathrm{i}} \qquad (28)$$

where $q_i(x,y)$ are the second-order shape functions, $N_i(x,y)$ are linear shape functions, NN_q is the number of nodes corresponding to $q_i(x,y)$, NN_L is the number of nodes corresponding to $N_i(x,y)$.

We should note that as a result of Newton's linearization, the additional terms appearing in the linearized equations are approximated as follows:

$$\boldsymbol{v}_{\mathrm{f}}^{o}=\sum_{i=1}^{NN_q} q_i(x,y)\boldsymbol{u}_{\mathrm{i}}^{o}\ ,\qquad \boldsymbol{D}^{o}=\sum_{i=1}^{NN_q} q_i(x,y)\boldsymbol{D}_{\mathrm{i}}^{o}\ ,$$

$$\boldsymbol{T}_1^{o}=\sum_{i=1}^{NN_q} q_i(x,y)\boldsymbol{S}_{\mathrm{i}}^{o}\ ,\qquad p^{o}=\sum_{i=1}^{NN_L} N_i(x,y)p_{\mathrm{i}}^{o}$$

$$\frac{\partial \boldsymbol{v}_{\mathrm{f}}^{o}}{\partial \boldsymbol{x}}=\sum_{i=1}^{NN_q}\frac{\partial q_i(x,y)}{\partial x}\boldsymbol{u}_{\mathrm{i}}^{o}\ ,\ \frac{\partial \boldsymbol{v}_{\mathrm{f}}^{o}}{\partial \boldsymbol{y}}=\sum_{i=1}^{NN_q}\frac{\partial q_i(x,y)}{\partial y}\boldsymbol{u}_{\mathrm{i}}^{o}\ ,\ \text{etc.} \qquad (29)$$

In our work, only bi-dimensional flows are considered. Therefore the problem consists of finding a velocity field $\boldsymbol{u}$=(u (x,y),v(x,y)), a pressure field p(x,y) and two tensor fields $\boldsymbol{S}$(x,y), and $\boldsymbol{D}$(x,y). The choice of the polynomial approximations for the variables $\boldsymbol{u}$, p, $\boldsymbol{S}$, and $\boldsymbol{D}$ requires careful attention. Since the early days of the numerical simulation of viscoelastic flows, it has been clear that some choices were better than others were.

In this research, the flow domain Ω, is discretized by means of quadrilateral finite elements. The velocity $\boldsymbol{u}$, polynomial stress $\boldsymbol{S}$ and rate of strain tensor $\boldsymbol{D}$ are approximated by continuous biquadratic (9 nodes) polynomials, while the pressure p is approximated by linear (4 nodes) polynomials. This choice satisfies the Babuska-Brezzi condition for the velocity-pressure-stress mixed finite element formulation with a P^2-C^0 interpolation for $\boldsymbol{u}$, $\boldsymbol{S}$, and $\boldsymbol{D}$, and a P^1-C^0 interpolation for p. This element is called EVSS-2, while in the EVSS-1 finite element approximation, p, $\boldsymbol{S}$, and $\boldsymbol{D}$ is P^1-C^0; it is P^2-C^0 for $\boldsymbol{u}$. EVSS-1 and EVSS-2 elements are depicted in Figure 1.

The integration over the flow region Ω is evaluated by the three-point tensor product Gaussian quadrature.

Define the vector of unknowns $\boldsymbol{q}$, such that

$$\boldsymbol{q}^{\mathrm{T}}\equiv(\boldsymbol{u},\boldsymbol{S},\boldsymbol{D},p) \qquad (30)$$

and the nonlinear residual vector $\boldsymbol{R}$ represented by

$$\boldsymbol{R}^{\mathrm{T}}=\boldsymbol{R}(\boldsymbol{u},\boldsymbol{S},\boldsymbol{D},p) \qquad (31)$$

Then the Newton's method described in the previous section requires the following equation be solved

$$\boldsymbol{J}(\boldsymbol{q}^{n})\Delta\boldsymbol{q}^{n+1}=-\boldsymbol{R}(\boldsymbol{q}^{n}) \quad \text{or}$$

$$\begin{pmatrix}\boldsymbol{J}_{11} & \boldsymbol{J}_{12} & \boldsymbol{J}_{13} & \boldsymbol{J}_{14}\\ \boldsymbol{J}_{21} & \boldsymbol{J}_{22} & \boldsymbol{J}_{23} & 0\\ \boldsymbol{J}_{31} & \boldsymbol{J}_{32} & \boldsymbol{J}_{33} & 0\\ \boldsymbol{J}_{41} & 0 & 0 & 0\end{pmatrix}^{n}\Delta\begin{pmatrix}\boldsymbol{u}\\ \boldsymbol{S}\\ \boldsymbol{D}\\ p\end{pmatrix}^{n+1}=-\begin{pmatrix}\boldsymbol{R}_M(\boldsymbol{u},\boldsymbol{S},\boldsymbol{D},p)\\ \boldsymbol{R}_S(\boldsymbol{u},\boldsymbol{S},\boldsymbol{D})\\ \boldsymbol{R}_D(\boldsymbol{u},\boldsymbol{D})\\ \boldsymbol{R}_C(\boldsymbol{u})\end{pmatrix} \qquad (33)$$

$$\Delta\boldsymbol{q}^{n+1}=\boldsymbol{q}^{n+1}-\boldsymbol{q}^{n}$$

Here **J** is the Jacobian (or the tangent) matrix and it's element J_{ij} is defined as $J_{ij}=\partial R_i/\partial q_j$, n is the iteration counter. Details of the finite element equations can be found in reference [6]

Solution Methods: Solver

The finite element discretizations described in the preceding chapter lead to large systems of equations that need to be solved in an efficient manner. Because the mathematical model is non-linear, at each non-linear step of the finite element procedure, we have the task of solving a large linear equation system:

Ax = b (34)

where **A** is a $N \times N$ general matrix. The size of the system ranges from $N = 5{,}000$ for small test problems to $N = 300{,}000$ or more for some of the mixed velocity-pressure-stress formulation problems. Only in the lower part of this spectrum, the direct solution techniques are feasible on contemporary computers. For larger problems, the memory limitations, as well as rapidly increasing computing time, make iterative solution techniques a necessity. It is therefore tempting to abandon the direct solver entirely, for the sake of code uniformity.

In an effort to reduce the cost required to solve a large linear system, we often lower our sights from the exact solution and become content with a solution which approximates the exact one with a prescribed accuracy. The iterative methods achieve this aim by constructing a series of guesses approximating the true solution.
To solve our equations iteratively, both sides of equations have to be multiplied by a matrix as shown in the following equation.

$$\boldsymbol{Q}^{-1}\boldsymbol{J}\Delta\boldsymbol{q} = \boldsymbol{Q}^{-1}(\boldsymbol{-R})$$

$\boldsymbol{Q}$ is called the pre-conditioner of the system. A pre-conditioner should possess the following properties:

1. $\boldsymbol{Q}$ is an approximation to $\boldsymbol{J}$
2. $\boldsymbol{Q}$ is easily factored so that for any right-hand side factor z, $\boldsymbol{Qy}=z$ can be solved easily.
3. $\boldsymbol{Q}^{-1}\boldsymbol{J}$ is a better conditioned matrix than $\boldsymbol{J}$.
4. $\boldsymbol{Q}$ needs a small space to store.

*The Generalized Minimal Residual (*GMRES*) scheme*

The GMRES method is designed to minimize the residual vector $\boldsymbol{r}$ in the Krylov subspace and $\boldsymbol{r}$ is defined same as in BiStabCG method. In the CG method the residual vectors $\boldsymbol{r}^{(0)}$, $\boldsymbol{r}^{(1)}$, $\boldsymbol{r}^{(2)}$, $\boldsymbol{r}^{(3)}$,…, $\boldsymbol{r}^{(n)}$ form an orthogonal basis for the space span $\{\boldsymbol{r}^{(0)}, \boldsymbol{Ar}^{(1)}, \boldsymbol{Ar}^{(2)}, \boldsymbol{Ar}^{(3)},\ldots, \boldsymbol{Ar}^{(n)}\}$. In the GMRES method, this basis is formed explicitly through the Gram-Schmidt orthogonalization. An efficient procedure to carry out the GMRES method was developed by Saad and Schultz [5]. It is given as follows:
Step 0: Construct a preconditioner $\boldsymbol{Q}$ for a linear system of equations $\boldsymbol{Ax}=\boldsymbol{b}$ and $\boldsymbol{Q}^{-1}\boldsymbol{Ax}=\boldsymbol{Q}^{-1}\boldsymbol{b}$
Step 1: Solve $\boldsymbol{Qx}^{(0)}=\boldsymbol{b}$ for $\boldsymbol{x}^{(0)}$
Step 2: Compute $\boldsymbol{r}^{(0)}=\boldsymbol{b}-\boldsymbol{Ax}$, $\beta = \left\|\boldsymbol{r}^{(0)}\right\|_2$ and $\boldsymbol{v}^{(1)} = \boldsymbol{r}^{(1)} / \beta$;
Step 3: For j=0,1,2,….m, carry out the following computations
3.1 $h_{i,j} = (\boldsymbol{Q}^{-1}\boldsymbol{Av}^{(j)}, \boldsymbol{v}^{(i)})$, i=1,2,…,j;

3.2 $\tilde{\boldsymbol{v}}^{(j+1)} = \boldsymbol{Q}^{-1}\boldsymbol{Av}^{(j)} - \sum_{i=1}^{j} (h_{i,j}, \boldsymbol{v}^{(i)})$

3.3 $h_{j+1,j} = \left\|\tilde{\boldsymbol{v}}_{j+1}\right\|_2$;

3.4 $\boldsymbol{v}^{(j+1)} = \tilde{\boldsymbol{v}}^{(j+1)} / h_{j+1,j}$;

Define $\mathbf{H}_m$ as the (m+1) x m upper Hessenberg matrix whose nonzero entries are coefficients $h_{i,j}$.
Step 4: Form an approximate solution $\boldsymbol{x}^{(m)} = \boldsymbol{x}^{(0)} + \boldsymbol{V}_m \boldsymbol{y}^{(m)}$,
where $\boldsymbol{V}_m \equiv [\, \boldsymbol{v}_1 \boldsymbol{v}_2 \boldsymbol{v}_3 \ldots \boldsymbol{v}_m \,]^{\mathrm{T}}$;
$\boldsymbol{y}^{(m)} = \min_i \|\beta \boldsymbol{e}_1 - \mathbf{H}_m \boldsymbol{y}^{(i)}\|_2$ and $\boldsymbol{e}_1 \equiv (1\ 0\ \cdots\ 0)^{\mathrm{T}}$
Step 5: Compute $\boldsymbol{r}^{(m)}=\boldsymbol{b}-\boldsymbol{A}\,\boldsymbol{x}^{(m)}$
Step 6: Check convergence $\left\|\boldsymbol{r}^{(m)}\right\|_2 \le RTOL\left\|\boldsymbol{r}^{(0)}\right\|_2 + ATOL$?
If not set $\boldsymbol{x}^{(0)} = \boldsymbol{x}^{(m)}$; compute $\boldsymbol{r}^{(0)}=\boldsymbol{b}-\boldsymbol{A}\,\boldsymbol{x}^{(0)}$,
$\beta = \left\|\boldsymbol{r}^{(0)}\right\|_2$ and $\boldsymbol{v}^{(1)} = \boldsymbol{r}^{(0)} / \beta$, return to Step 3.

It should be noted that the algorithm given above differs from the classical GMRES in two ways. In the classical GMRES, the Krylov space is continually expanded until convergence is reached. This leads to excessive memory requirements, and the advantage over a direct method of solution is lost. To alleviate this problem, in a practical GMRES algorithm, the dimension of the Krylov space m is limited a priori, and if this dimension proves insufficient, the algorithm is restarted in the next outer iteration. Alternatively, the orthogonalization process can be truncated to include only a given number of previous basis vectors, but this option is not pursued here. Unfortunately, these modified methods are not guaranteed to converge, and the

choice of restart frequency has to be made carefully, usually by numerical experimentation. The current algorithm also differs from other GMRES derivatives in that it allows variable preconditioning at each inner iteration. This feature enables us to freely mix two different but complementary preconditioners.

Preconditioning

In contrast to the direct methods of solution, the iterative schemes can be extremely sensitive to the particular numerical properties of the system matrix **A**, and the GMRES algorithm is no exception. The rate of convergence of Krylov subspace methods is influenced by the condition number of the matrix **A**. In our research, we used both ILU0 and ILUT preconditioners [6]. We performed a variety of numerical experimentations to determine the optimal Krylov subspace *m* and the best performance is observed when Krylov subspace *m* is chosen as 20. For high Deborah numbers, the GMRES algorithm with ILU0 preconditioner does not generate a convergent solution. The reason we believe is because the problem due to the diagonal dominance of the matrix system becomes worse as the convective terms become more dominant. We also implemented the diagonal preconditioner and the convergence problem associated with ILU0 preconditioner also occurred at high Deborah numbers. It is our experience via numerical experimentation that the GMRES solver together with ILUT preconditioner is the method of choice for solving the linear system of equations for the calculation of viscoelastic fluid flows.

4. RESULTS AND VALIDATION OF COMPUTATIONAL IMPLEMENTATION

The mixed finite element method described in the previous section was tested and validated on two classical benchmark problems with geometrical singularities. The current results are in excellent agreement with previously published results for viscoelastic fluid flows.

The two benchmark problems are: the stick-slip problem and the 4:1 contraction problem. There exists an abundant literature concerning these two problems. The difficulty of the 4:1 contraction problem comes from the geometric singularity at the re-entrant corner. For the stick-slip problem the difficulty comes from the passage from a Dirichlet boundary condition (stick) to a Neumann boundary condition (slip). We present the solutions for the following flow variables for each problem:

(a) The variation of horizontal velocity component: u
(b) The variation of vertical velocity component: v
(c) The variation of the pressure: p
(d) The variation of Newtonian contribution to the extra-stress component: rn
(e) The variation of Newtonian contribution to the extra-stress component: sn
(f) The variation of Newtonian contribution to the extra-stress component: tn
(g) The variation of polymeric contribution to the extra-stress component: r
(h) The variation of polymeric contribution to the extra-stress component: s
(i) The variation of polymeric contribution to the extra-stress component: t

The parameters of the flow and the constitutive models are summarized in the following table:

Ratio	0.11
Density	1000 Kg/m^3
Viscosity	1000 Pa.s
α_{GL} :Giesekus-Leonov Model parameter	0.5
ε_{PTT}: PTT model parameter	0.1

Table 1. The parameters used in calculations

The Stick-Slip Problem

The stick-slip geometry is depicted in Figure 2. A viscoelastic fluid flows in a planar channel of half width *H* and length 2*L*. The channel is taken to have no-slip surfaces for $x \leq 0$ and shear free surfaces for $x > 0$. The velocity field at the entrance and the exit are assumed to be fully developed. The flow at the outlet is simply a rigid motion at a dimensionless velocity of 1/3. The centerline is a plane of symmetry.

The boundary conditions used in the analysis and calculations are

$u(x, 1) = v(x,2) = 0, \qquad -\Lambda \leq x \leq \Lambda,$

$S_{yx}(x, 1) = 0, \quad -\Lambda \le x \le \Lambda,$
$u(x, 2) = 0, \quad -\Lambda \le x \le 0,$
$S_{yx}(x, 2) = 0, \quad 0 \le x \le \Lambda,$
$u(-\Lambda, y) = \phi(y), \; u(\Lambda, y) = 1/3, \; v(-\Lambda, y) = v(\Lambda, y) = 0,$

where Λ, is the dimensionless length of the upstream and downstream sections of the channel and $\phi(y)$ is the fully developed velocity profile in the upstream section of the channel given by $0.5((y/2)-(y/2)^2)$.

We compare our results with Apelian et al. [7] for Deborah number De=0.6, where $De=3\lambda_1 V/H$, V is the average of the inlet velocity in the channel and it is 1/3. Since H=1.0, $De=\lambda_1$. Figure 2a shows the finite element mesh used in calculation. The number of elements is 360, the number of equations is 12,603, the number of pressure nodes is 403 and the number of nonzero elements of the Jacobian matrix for the compressed sparse row format is 1,543,583. In Figure 2b, the present results for the axial velocity profile for the UCM model along the centerline $(y=1)$ and along the wall $(y=2)$ is plotted. Our results are in excellent agreement with those of Apelian et al. [3] as can be seen from Figure 2b.
The calculations are obtained for De = 0.5 for all of the models. The results are plotted in Figures 3a-i

The 4:1 Contraction Problem
The geometry of the problem and the boundary conditions are presented in Figure 4. Previous calculations have shown that the plane flow through a 4:1 contraction of an Oldroyd-B fluid is not very stimulating from a numerical point of view because the main features of the flow are minimally affected by the amount of the elasticity. Such an absence of deviation from the Newtonian behavior for a planar 4:1 contraction has been confirmed experimentally as long as the flow remains symmetric with respect to the geometrical plane of symmetry. In our calculations, the flow is constrained to be symmetric, and one would not expect dramatic modifications of the streamlines. We also simulated the other popular models (i.e. UCM, PTT and Giesekus Models) for the sake of completeness.
To analyze the flow, we have selected a mesh of quadrilateral finite elements (Figure 4b). The non-dimensional downstream length equals 50, while the upstream length equals 20. The number of elements is 580, the number of equations is 20,577, the number of pressure nodes is 665 and the number of nonzero elements of the Jacobian matrix for the compressed sparse row format is 2,482,205. The boundary conditions are the usual ones, i.e. imposed stress components in the entry section and imposed velocity components in the entry sections. The fluid is of the Oldroyd-B type with a ratio β=0.11. The Deborah number De is the product of $\lambda_1\gamma_w$, where γ_w is measured on the wall in the downstream fully developed flow. The calculations are advanced with an 0.3 interval of De number increment and convergent solutions are obtained for De = 2.25 which is higher than one previously reported in the literature [8] which is De = 2.0 with a SUPG formulation. We believe that the reason for this is because of our EVSS-2 implementation to the flow problem. The results are given along the line of singularity (y=1).
Again, first we compare our results with Marchal and Crochet [8] for horizontal and vertical velocity components at De=2.0 along x=0.9 line (Figure 4c) by setting porosity to unity which is the case of the pure viscoelastic fluid flow. Our results exactly match those of Marchal and Crochet [4] as can be seen in Figure 4c.
The calculations are carried out at De = 1.5 when the inertia is present in the flow filed. We use the same value of the density as for the Stick-Slip problem. The solutions are plotted in Figures 5.a – i.

5. CONCLUSIONS
In this research, both Newtonian and viscoelastic constitutive equations are solved using the consistent finite element formulation. The latter included Elastic-Viscous-Split-Scheme (EVSS) formulation of upper-convected Maxwell, Oldroyd-B, Giesekus-Leonov and Phan-Tien Tanner Models characterizing the behavior of viscoelastic fluids.

We consider a computational method capable of effectively solving incompressible viscoelastic fluid flows for the problems with strong singularities. The mixed finite element formulation utilizing Newton's linearization, SUPG method and EVSS-2 discretization is introduced and explained in detail. Then we started with a brief review of direct solvers. Recognizing the excessive cost of the direct solution, we moved on to the iterative methods in general and the Generalized Minimum Residual method in particular. An efficient version of this algorithm was recounted and the issues of convergence and preconditioning touched upon. We described our experience in this area, stemming from the implementation of the GMRES method on viscoelastic fluid flows.

Finally, the results for two benchmark problems with strong singularities are presented. Computations have been performed with the aid of numerical methods described so far. For the Stick-Slip problem, we first obtained the solutions for a Newtonian fluid. Then, simulations for viscoelastic models are performed for up to Deborah number of 0.6 without including the inertia. The effects of the inertia are also included for De=0.5 for all of the viscoelastic models. As a second test problem, we considered the 4 to 1 contraction problem. Following the same steps as in the Stick-Slip problem, we first validated our results, then the results are given for Newtonian, UCM, Oldroyd-B, PTT and Giesekus-Leonov fluids for the Deborah numbers of up to 0.0, 0.3, 0.9, 1.5, 2.25. Also inertia is included for the case of De = 2.25. Our results showed that there are discrepancies between the viscoelastic model for high De number simulations, especially Giesekus-Leonov model shows different behavior of stress field than others, while the other three models are in reasonable agreement.

REFERENCES

[1] R. B. Bird, R. C. Armstrong, O. Hassager. "Dynamics of Polymeric Liquids, Vol. 1, Fluid Mechanics ", *2nd ed.,* Wiley Interscience, 1987.

[2] A.N. Brooks and T.J.R. Hughes. "Streamline upwind/Petrov-Galerkin formulations for convection dominated flows with particular emphasis on the incompressible Navier-Stokes equations", *Comput. Methods Appl. Mech. Eng.*, 32:199, 1982

[3] F. Shakib. "Finite element analysis of the compressible Eular and Navier-Stokes equations", *Ph.D. Dissertation*, Stanford University, 1989.

[4] R.C. King, M.R. Apelian, R.C. Armstrong and R.A. Brown. "Numerically stable finite element techniques for viscoelastic calculations in smooth and singular geometries", *J. Non-Newtonian Fluid Mech.*, 29:147-216, 1988

[5] Y. Saad and M.H. Schulz. "GMRES: A generalized minimal residual algorithm for solving nonsymmetric linear system", *SIAM, J. Sci. Statist. Comput.*, 7:856-869, 1986

[6] B. Alakus. "Finite element computations of viscoelastic fluid flows employing quasi-linear and nonlinear models", *Ph.D. Dissertation*, The University of Minnesota, 2001.

[7] M.R. Apelian, R.C. Armstrong and R.A. Brown. "Impact of the constitutive equation and singularity on the calculation of Stick-Slip flow: The modified upper-convected Maxwell model (MUCM)", *Journal of Non-Newtonian Fluid Mechanics*, 27:299-321, 1988

[8] J.M. Marchal and M.J. Crochet. "A new mixed finite element for calculating viscoelastic flow" *Journal of Non-Newtonian Fluid Mechanics*, 26:77-114, 1987

FIGURES

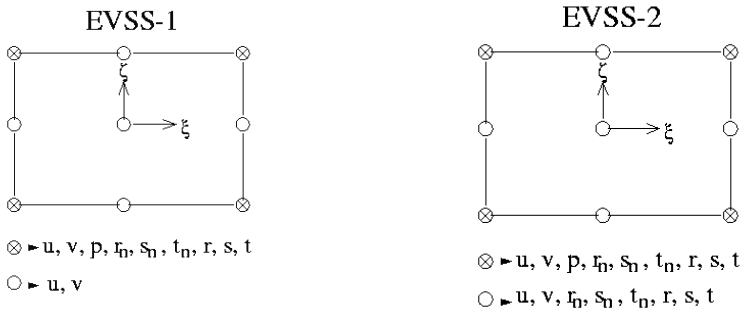

Figure 1. EVSS-1 and EVSS-2 elements and approximation spaces.

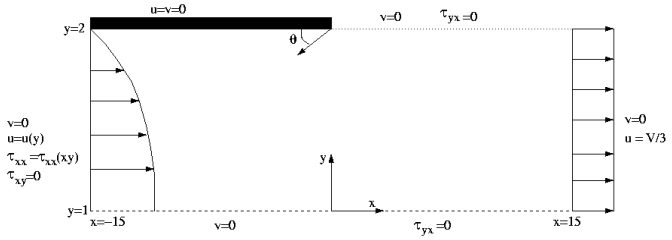

Figure 2 Geometry for planar 2 dimensional stick-slip flow.

Figure 2a Finite element mesh for the stick-slip problem

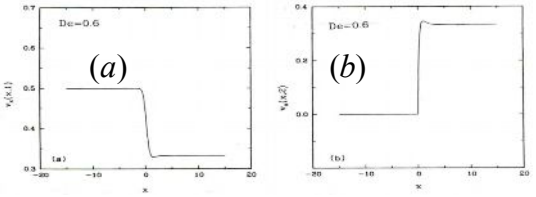

Figure 2a) Axial Velocity Profile of Apelian et al. [7]
(a)Axial velocity profile for the UCM model at De = 0.6 along the centerline (y = 1)
(b) Axial velocity profile for the UCM model at De = 0.6 along the wall (y = 2)

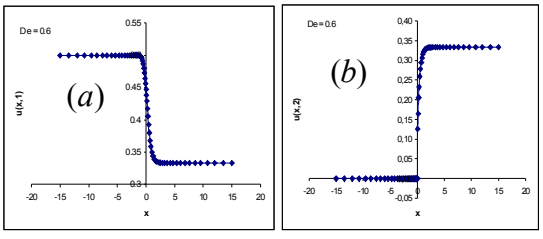

Figure 2b) Axial Velocity Profile (Present Results)
(a) Axial velocity profile for the UCM model at De = 0.6 along the centerline (y = 1)
(b) Axial velocity profile for the UCM model at De = 0.6 along the wall (y = 2)

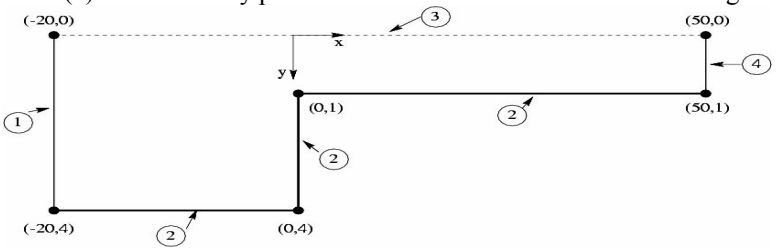

Figure 4a The 4:1 contraction problem
geometry and boundary conditions: (1) Poisseuille flow for velocity and extra stress tensor, (2) no-slip walls (3) symmetry line (4) fully developed profile

Figure 4b The finite element mesh for the 4:1 contraction problem

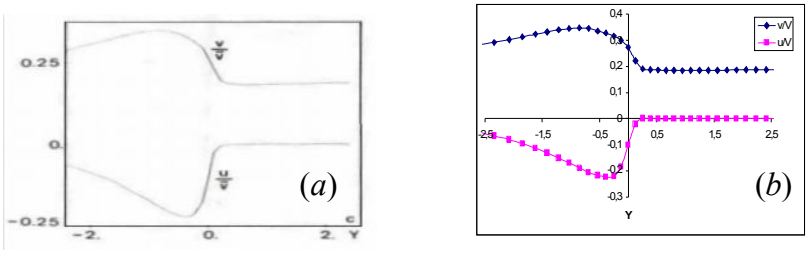

Figure 4c-a Horizontal and vertical velocity components at De = 2.0 along the x = 0.9 line [8]
Figure 4c-b Horizontal and vertical velocity components at De = 2.0 along the x = 0.9 line (Present Results)

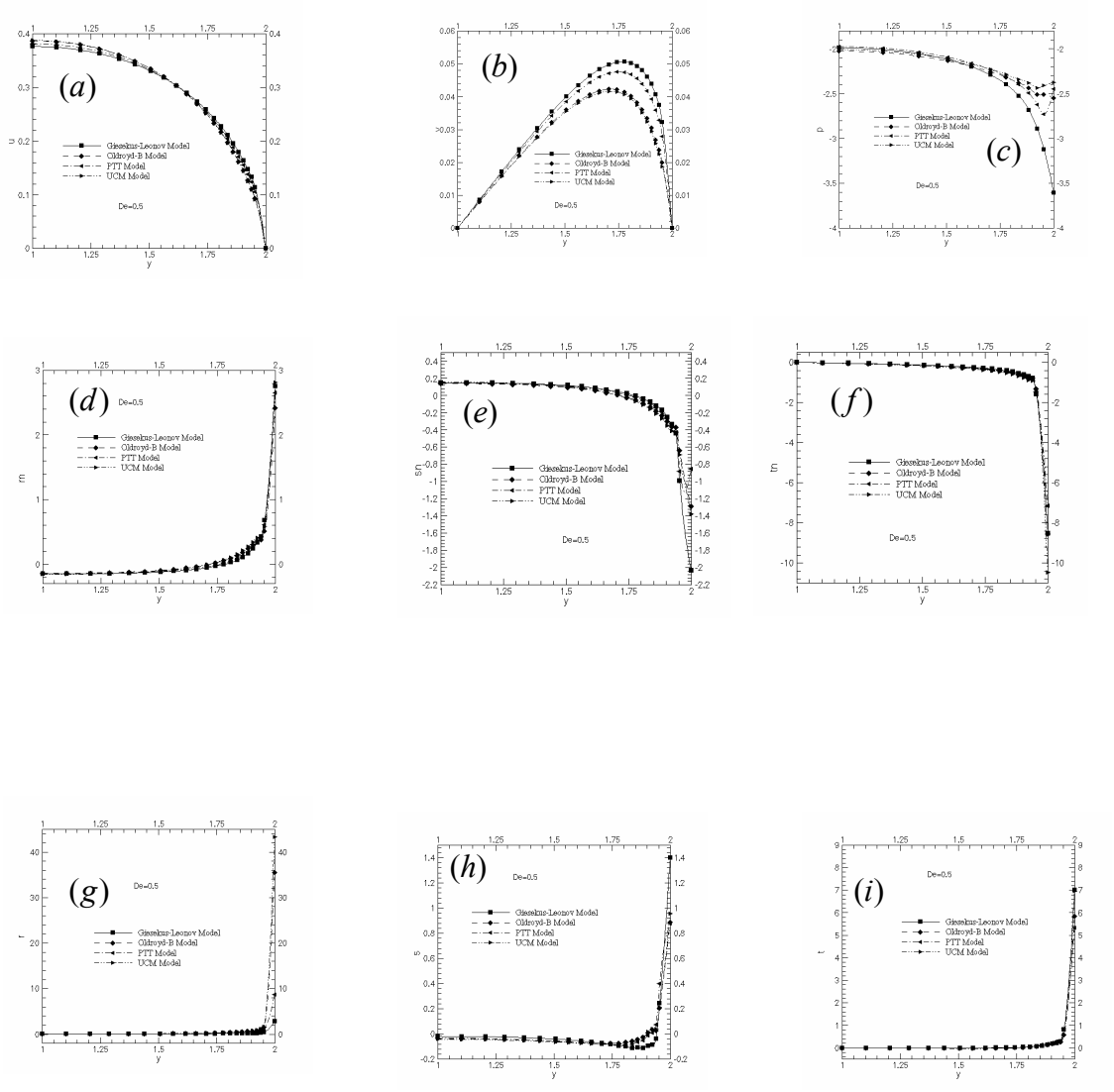

Figure 3a- i) Solution for the Stick-Slip problem for De = 0.5 along the centerline *(*x = 0)

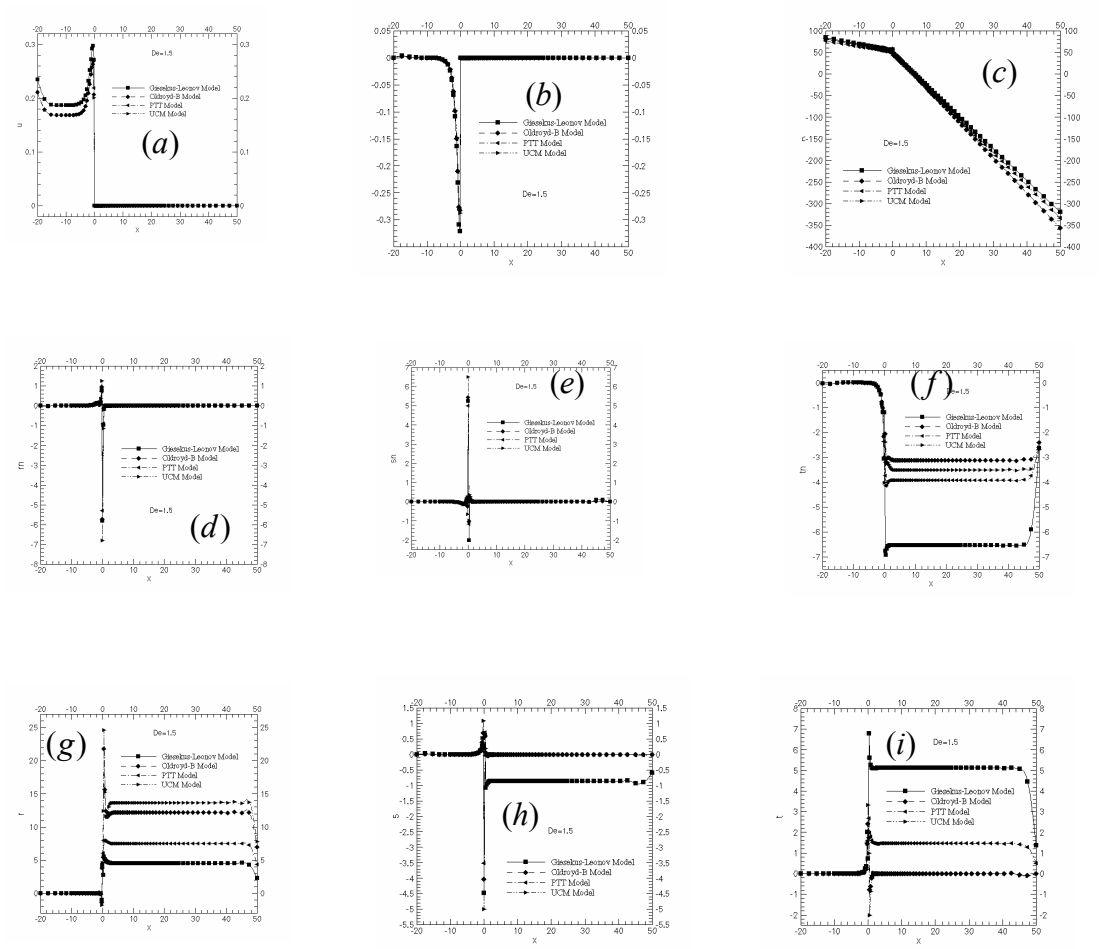

Figure 5a- i) Solution for the Contraction problem for De = 1.5 along (y = 1)